FLUID STRUCTURE INTERACTION BASED ON PANEL METHOD AND GEOMETRICALLY NONLINEAR STRUCTURAL ANALYSIS

Sedat Özöztürk[1], Altan Kayran[2], İsmail H. Tuncer[3]

Department of Aerospace Engineering
Middle East Technical University, 06531, Ankara, Turkey

ABSTRACT

The article presents fluid-structure interaction methodology for the static aeroelastic coupling of aerostructures. A CFD and a FEM solver are coupled and the aeroelastic solution is iterated in order to obtain the steady state condition of the aerostructure. A three dimensional panel method is used as the CFD solver and MSC.Nastran is used as the finite element solver. In order to investigate large deflection effects, which are common in flexible aerostructures such as high aspect ratio wings, panel solution is coupled with both geometrically linear and nonlinear solution sequences of Nastran. The article explains the coupling process of the aerodynamic panels and the structural finite element mesh in detail and emphasizes the significance of geometrically non-linear structural analysis in static aeroelastic analysis of flexible structures.

INTRODUCTION

The aerodynamic forces on an aerostructure depend on its geometric configuration. Deflections and displacements of the structure are caused by the aerodynamic forces. This coupling may results in aeroelastic phenomena such as load redistribution, static divergence and flutter for an aero-structure. There are simple and fast tools to perform aeroelastic analysis such as MSC. Nastran structural finite element solver [MSC Nastran Quick Reference Guide, 2014] coupled with MSC.Nastran aeroelasticity module [MSC Nastran Aeroelastic Analysis User's Guide, 2010]. MSC.Nastran aeroelasticity module has three different solution sequences for the static aeroelasticity, flutter and dynamic response. Aeroelasticity module of Nastran uses doublet lattice method for aerodynamic calculations, and it produces accurate results for low air speed and structures undergoing small deflections and all non-linearities related to the flow and the structure are not considered. However, nonlinearities can be important in calculating the static and dynamic aeroelastic response of especially flexible structures that undergo usually large deflections. Wind turbines, helicopter blades, high aspect ratio UAVs, hybrid powered long endurance UAVs, HALE with very flexible wings (e.g. Helios) are some examples of flexible structures. M. J. Patil and D. H. Hodges [Patil and Hodges, 2006] analyzed large aircraft motion coupled with geometrically nonlinear structural deflection and generated results for a typical high aspect-ratio "flying wing" configuration. They claim that the aircraft undergoes large deflection during trim. The flight dynamic characteristics of the deformed aircraft are completely different as compared to the rigid aircraft. Palacios and Cesnik [Palacios and Cesnik, 2005] performed fluid structure interaction solution based on nonlinear structural dynamics and compressible unsteady aerodynamics for high fidelity analysis of HALE aircraft. In their study, the static nonlinear aeroelastic response of a 16:1 half-aspect ratio wing is investigated for steady flight conditions.

[1] Ph.D student in Aeroepace Eng. Dept, Email: e139609@metu.edu.tr
[2] Prof. in Aerospace Engineering Department, Email: akayran@metu.edu.tr
[3] Prof. in Aerospace Engineering Department, Email: ismail.h.tuncer@ae.metu.edu.tr

In the present study, a 3D panel code is coupled with the geometrically nonlinear finite element solver and static aeroelastic solution is obtained for flexible structures. In both computational aerodynamics and computational mechanics sophisticated tools of different fidelity are available. Combining computational aerodynamics and computational mechanics tools in an aeroelastic analysis framework is a frequently applied method. Considering the increased use of flexible aero-structures in different applications in the aerospace industry, including geometrically non-linear structural analysis in aeroelastic analysis becomes inevitable. Geometric non-linearity not only affects the distribution of the loads different from the load distribution that would be obtained using linear structural analysis in aeroelastic analysis, but also aeroelastic instability speeds are also significantly affected. This study explains the coupling process of the aerodynamic panels and the structural finite element mesh in detail and emphasizes the significance of geometrically non-linear structural analysis in static aeroelastic analysis of flexible structures.

METHOD

Flow solution

In this study, 3D panel code Apame [Aircraft 3D Panel Method web site, 2015] is used as the CFD solver. Panel method is not capable to predict boundary layer, flow seperation and supersonic flow cannot be modeled by panel method. However, it is fast and accurate for subsonic, high Reynolds number and attached flow.

Structural finite element solution

For the structural finite element solution MSC. Nastran is used. For linear analysis solution sequence 101 of Nastran is used to solve for the deflections and for geometrically non-linear solution, solution sequence 400 is used.

Force Mapping Method

In aeroelastic analysis, panel and FEM mesh are usually not matched. Therefore, proper transfer of the forces from the panel solution to the structural finite element model is required. In this study, isoparametric mapping method is applied in order to transfer forces from panel mesh to FEM mesh [Samareh, 2007; Akenine-Möller, 2001; Ahmed, 2006]. Isoparametric mapping method uses shape functions for mapping and is capable of interpolation [Ahmed, 2006]. Parametric locations of panel nodes on FEM elements are calculated by inverse parametric transformation [Hua, 1990] and shape function values at these parametric locations are used to form the mapping matrix. The method maps force values on each panel node to the corresponding finite element in the structural mesh, and shape functions are used to distribute force to nodes of corresponding finite element. The method guarantees conservation of force and moment [Samareh, 2007].

Figure 1 shows a quadrilateral isoparametric element in global and parametric coordinate systems. Parametric location of panel node P should be known in order to implement isoparametric mapping method. There is not any direct solution to find the parametric location of Point P. However, Hua suggests inverse transformation solution sets for different conditions given in Table 1.

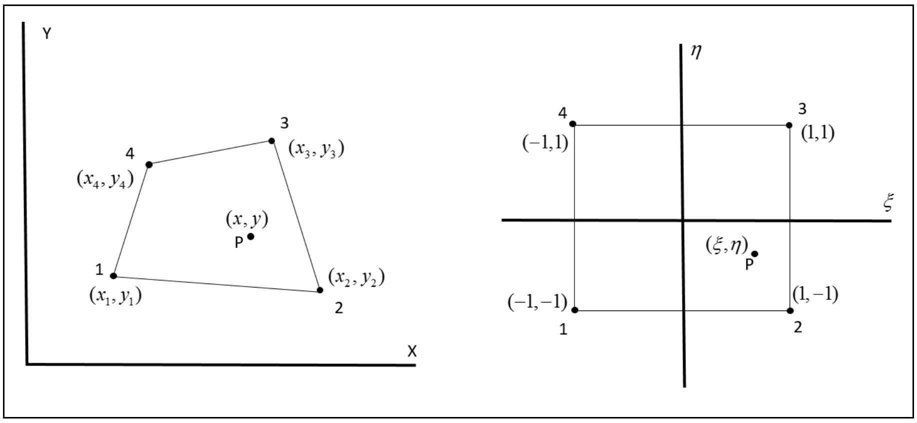

Figure 1: *A quadrilateral isoparametric element in global and parametric coordinate systems*

Table 1: *Solutions for inverse transformations*

No	Condition	Solution
1	$a_1 a_2 a_b a_c \neq 0$	$a_b \xi^2 + (c_b + d_a)\xi + d_c = 0$
2	$a_1 = 0 \text{ and } a_2 c_1 \neq 0$	$\eta = (a_d + b_a \xi) / a_c$
3	$a_2 = 0 \text{ and } a_1 b_2 \neq 0$	$\text{where } \xi \in [-1.0, +1.0]$
4	$a_1 a_2 \neq 0 \text{ and } a_b = 0$	$\xi = (a_1 d_c) / (b_1 a_c + a_1 a_d); \quad \eta = a_d / a_c$
5	$a_1 a_2 \neq 0 \text{ and } a_c = 0$	$\xi = a_d / a_b; \quad \eta = (a_1 d_b) / (c_1 a_b + a_1 a_d)$
6	$\text{All other conditions}$	$\xi = d_c / (a_1 d_2 + b_c); \quad \eta = b_d / (a_2 d_1 + b_c)$

where;

$$\begin{bmatrix} a_1 & a_2 \\ b_1 & b_2 \\ c_1 & c_2 \end{bmatrix} = \begin{bmatrix} -1 & +1 & -1 & +1 \\ +1 & +1 & -1 & -1 \\ -1 & +1 & +1 & -1 \end{bmatrix} \begin{bmatrix} x_1 & y_1 \\ x_2 & y_2 \\ x_3 & y_3 \\ x_4 & y_4 \end{bmatrix} \tag{1}$$

$$\begin{aligned} d_1 &= 4x - (x_1 + x_2 + x_3 + x_4) \\ d_2 &= 4y - (y_1 + y_2 + y_3 + y_4) \end{aligned} \tag{2}$$

and a compact notation to represent the determinant of the 2 x 2 matrix is shown as:

$$r_s = \begin{vmatrix} r_1 & s_1 \\ r_2 & s_2 \end{vmatrix} = r_1 s_2 - r_2 s_1; \qquad r, s = a, b, c, d \tag{3}$$

Bilinear shape functions for the four nodes of the elements are given by Equation 4:

$$\begin{aligned} N_1 &= \frac{1}{4}(1-\xi)(1-\eta) \qquad & N_2 &= \frac{1}{4}(1+\xi)(1-\eta) \\ N_3 &= \frac{1}{4}(1+\xi)(1+\eta) \qquad & N_4 &= \frac{1}{4}(1-\xi)(1+\eta) \end{aligned} \tag{4}$$

Force (F_P) at point P can be mapped to FEM element nodes utilizing Equation 5.

$$\begin{aligned} F_1 &= F_P \cdot N_1(\xi_P, \eta_P) \\ F_2 &= F_P \cdot N_2(\xi_P, \eta_P) \\ F_3 &= F_P \cdot N_3(\xi_P, \eta_P) \\ F_4 &= F_P \cdot N_4(\xi_P, \eta_P) \end{aligned} \tag{5}$$

Structural Analysis

Structural analysis is performed by MSC.Nastran. In this article, SOL101 (Linear Static Analysis) and SOL400 (Non-Linear Static Analysis) modules of MSC.Nastran are used as the structural finite element solver and the effect of geometric non-linearity is investigated.

Linear static analysis assumes deflections are small and stiffness is constant and does not change with the deflection of the structure. However, flexible aero structures may be exposed to large deflections and stiffness of the structure changes when the structure is deformed. Therefore, geometrically non-linear analysis is performed by the non-linear analysis module of Nastran.

Displacement Mapping Method - Surface Spline Method

Displacement mapping method used in the present study is based on the infinite plate spline method which is the most common deflection mapping algorithm in the literature [Smith, 1995]. Infinite plate spline method is based on small deflections theory of an infinite plate. Using solutions of the equilibrium equation for an infinite plate, a set of concentrated loads are calculated that give rise to the deflections at the data points. The concentrated forces are then substituted back into the solution providing a smooth surface that passes through the data.

The mathematical analysis involves the finding of the point loads at a set of points given the deflections at the same set of points by utilizing the vertical deflection solution of a plate due to a transverse point load. In a typical aeroelastic analysis, the set of know deflections would be the deflections at the structural grid points. For a set of *N* point loads the vertical displacement $w(x,y)$ of the infinite plate can be written as [Harder, 1972; MSC Nastran Aeroelastic Analysis User's Guide, 2010]:

$$w(x,y)=\sum_{i=1}^{N}\left(A_i+B_i r_i^2+(P_i/16\pi D)r_i^2\ln r_i^2\right) \tag{6}$$

where P_i are point loads applied at N number of points, A_i and B_i are the arbitrary constants, *D* is the bending stiffness of the plate and r_i is the distance from the i^{th} applied load to the point (*x,y*) where the vertical deflection is desired. It is stipulated that radial lines originating from the loaded points will appear to be straight lines at long distances from the applied loads. Therefore, to satisfy the boundary conditions at infinity Eqn. 6 is expanded for large radial distances from the origin and only the terms of order $x=r\cos\theta$, $y=r\sin\theta$, $\ln r^2$, 1 etc. are retained. After the simplifications, a general solution for the vertical displacement can be written as:

$$w(x,y)=a_0+a_1x+a_2y+\sum_{i=1}^{N}K_i(x,y)P_i \tag{7}$$

where a_0, a_1, a_2 are arbitrary constants and $K_i(x,y)=(1/(16\pi D))\,r_i^2\ln r_i^2$. The *N*+3 unknowns a_0, a_1, a_2 and P_i are determined from *N* known displacements of the structural grids and 3 equilibrium equations $\sum P_i=\sum x_iP_i=\sum y_iP_i=0$. Once all the unknowns in Eqn. 7 are determined, vertical displacements at the aerodynamic grid locations can be determined from Eqn. 7 by entering the (*x,y*) coordinates of the aerodynamic grids and finally these equations can be cast into the form given by Eqn. 8 completing the coupling of the structural and aerodynamic deflections.

$$\{u_a\}=[G_{as}]\{u_s\} \tag{8}$$

where the splining methods lead to an interpolation matrix $[G_{as}]$ that relates the components of structural grid point deflections $\{u_s\}$ to the deflections of the aerodynamic grid points $\{u_a\}$.

NUMERICAL RESULTS

Figure 2 shows the pressure distribution on the wing and mapped forces in the structural finite element mesh. The rectangular unswept wing structure that is used for the demonstration of the static aeroelastic coupling process has a wing span of 974 mm and 60 mm chord. There are 21 equally spaced ribs and single spar in the wing structure. Ribs are made up of 0.1mm thick steel and skin is 0.5mm steel. Spar is located at mid-chord and it is made up of 1.14mm thick steel. The airfoil is NACA0015, airspeed that is used in the aeroelastic analysis is taken as 100 m/s and angle of attack is 2.5°. There are 2394 CQUADR elements in the finite element model [MSC Nastran Quick Reference Guide, 2014]. CQUADR elements allow drilling degrees of freedom. All nodes at wing root are fixed at 6 dof. In the panel method, 8517 panels are used in the aerodynamic solution.

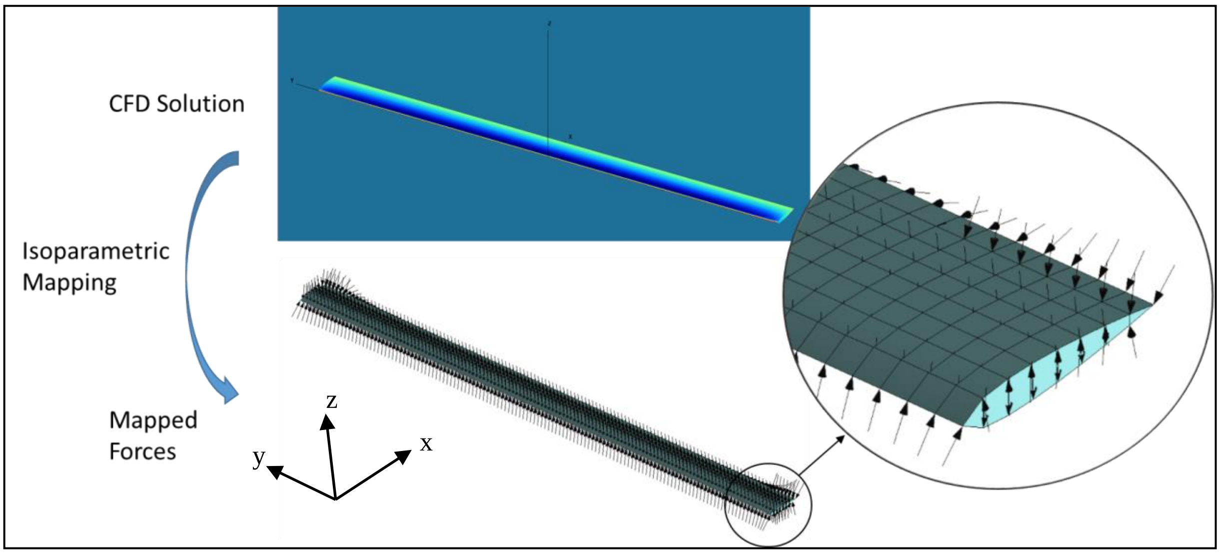

Figure 2: *Pressure distribution and mapped forces*

Table 2 shows the total force and total moment values before and after the mapping at the end of the first force mapping. In Table 2, *x* is the chordwise direction, *y* is the spanwise direction and z is the vertical diretion as shown in Figure 2. From Table 2, it can be seen that conservation of the force and the moment values are satisfied.

Table 2: *Total forces and moments after mapping*

		Fx (N)	*Fy (N)*	*Fz (N)*	*Mx (N.mm)*	*My (N.mm)*	*Mz (N.mm)*
Lower Skin	Before Mapping	8.31	-2.64E-7	-42.98	-1.08	938.94	-0.14
	After Mapping	8.31	-2.64E-7	-42.98	-1.08	941.51	-0.14
Upper Skin	Before Mapping	-10.71	2.13E-6	128.93	-1.33	-2217.35	9.82E-2
	After Mapping	-10.71	2.13E-6	128.93	-1.33	-2219.40	9.84E-2

Figure 3 shows the deformed shape of the wing structure obtained by the nonlinear finite element analysis under mapped aero loads at the end of the first iteration. At the end of the first iteration maximum tip displacement is calculated as 44mm.

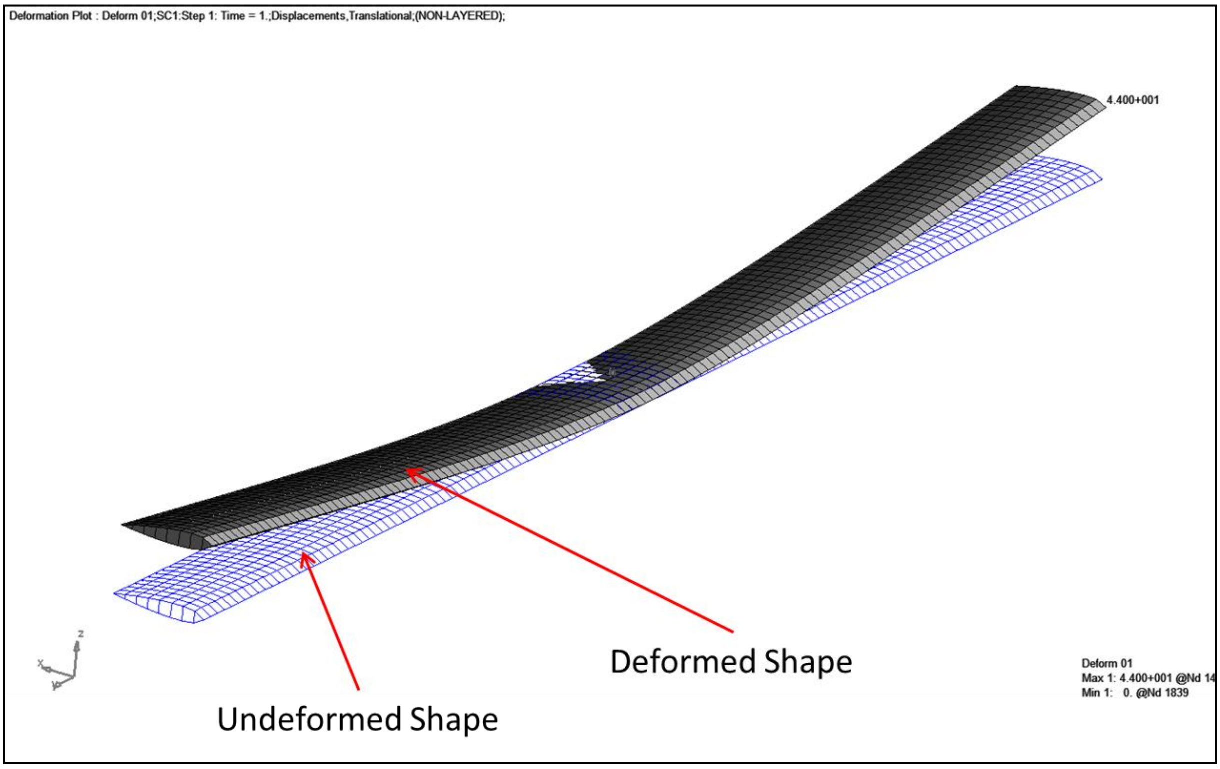

Figure 3: *Wing deflection obtained by nonlinear static analysis at the end of the first iteration*

Figure 4 shows the infinite plate spline method applied to the wing structure at the end of the first iteration. Deformed panel mesh in red color is obtained using the infinite spline method.

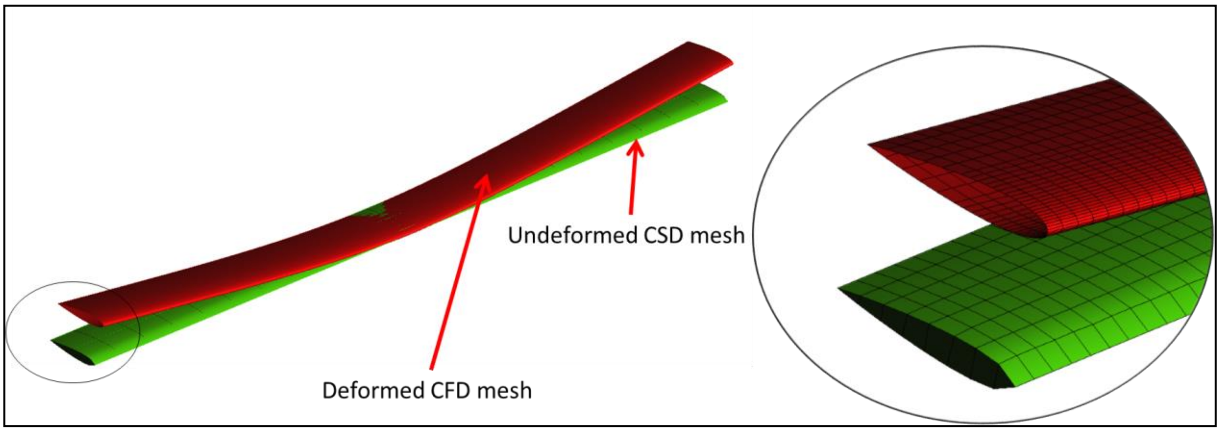

Figure 4: *Displacement splining for the wing structure at the end of the first iteration*

Figure 5 shows the change of the lift with the number of aeroelastic iterations performed in the coupled analysis. As it is seen, for the particular wing structure analyzed, lift converges in 20 iterations. Since magnitude of lift changes significantly with the iterations, it can be concluded that the particular wing studied is very flexible. In the converged configuration, geometrically non-linear structural analysis gives 350N total lift and geometrically linear structural analysis gives 550N total lift.

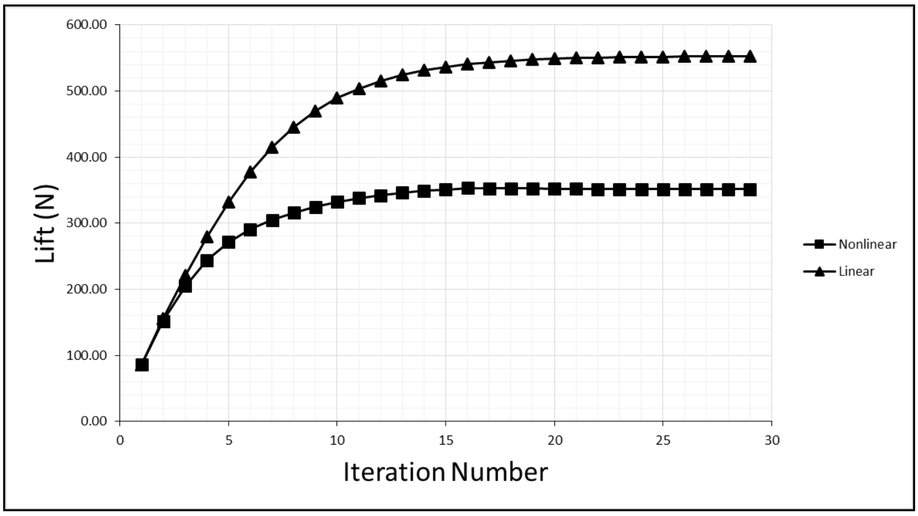

Figure 5: *Variation of lift with aeroelastic iterations*

Figure 6 shows variation of tip displacement with aeroelastic iterations. Geometrically nonlinear structural analysis converges to a lower tip displacement value than the linear analysis, as expected. It should be noted that for the 100 m/s airspeed, wing loading is high and tip displacement is almost 1/3rd of the wing span for the linear analysis. It should be noted that the demonstrative example is selected such that the wing structure undergoes large deflection. Large deflection could be due to wing flexibility for the particular airspeed selected or could be due to the airspeed which could be too high for the wing structure studied.

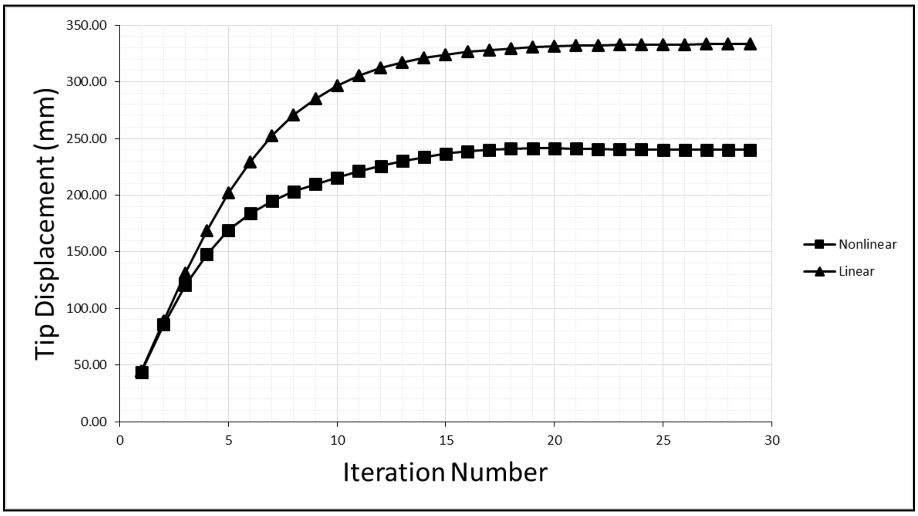

Figure 6: *Variation of tip displacement with aeroelastic iterations*

Figure 7 shows the one-to-one scale deformed shapes of the wing structure obtained by geometrically linear and nonlinear structural analyses.

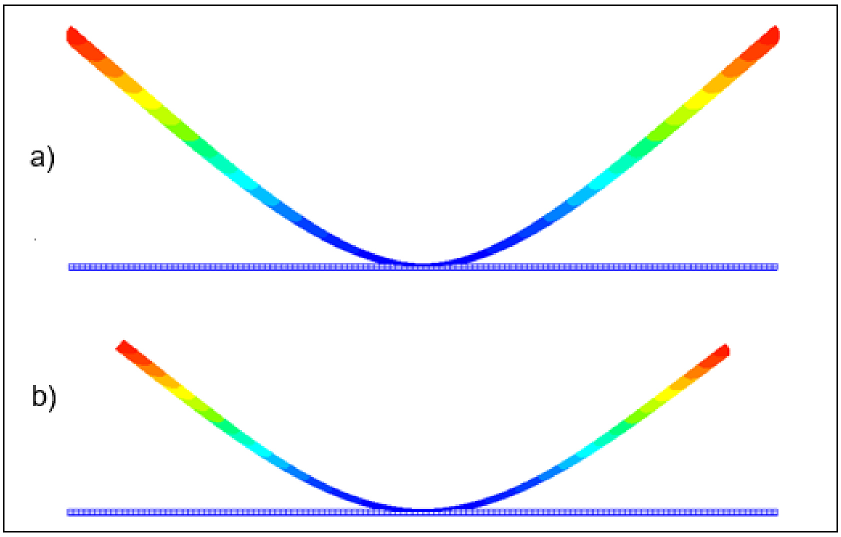

Figure 7: *True scale deformed shapes of the wing structure for a) Linear and b) Nonlinear solutions*

Figure 8 shows variation of converged tip displacements with airspeed. It is seen that linear and nonlinear solutions give same results at low speeds when the aerodynamic load is small. However, when airspeed is increased, linear and nonlinear solution results differs because of the large deflection effects.

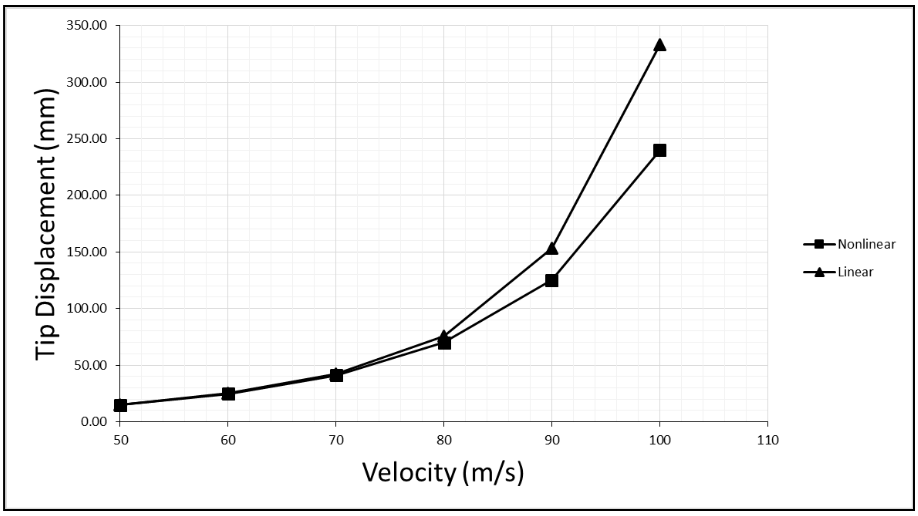

Figure 8: *Variation of converged tip displacement with airspeed*

CONCLUSION

The article explains the coupling process of the aerodynamic panels and the structural finite element mesh for the static aeroelastic analysis of aero structures. In order to investigate the large deflection effect, which is common in flexible aero-structures such as high aspect ratio wings, panel aerodynamics solution is coupled with both with geometrically linear and nonlinear solution sequences of Nastran. Results presented for the coupling process verifies the force and displacement mapping methods used. The effect of geometric nonlinearity is investigated in a high aspect ratio wing by making comparisons of the aeroelastic analysis results obtained with the use of geometrically linear and non-linear analysis in the coupled panel method structural finite element solution. For the demonstrative example, it is shown that once the convergence is achieved, aeroelastic analysis with geometrically non-linear structural analysis gives %57 lower lift compared to the aeroelastic analysis with geometrically linear structural analysis. Although the demonstrative example is a made-up problem, the results obtained show the significance of employing geometrically non-linear structural analysis in aeroelastic analysis of flexible structures. As shown in the present study, when geometrically linear structural analysis is used in aeroelastic analysis of flexible wing structures undegoing large deflections, the resultant lift force is highly overestimated. The study on the variation of converged tip displacement with airspeed showed that at low airspeeds using linear or nonlinear structural analysis in aeroelastic analysis results in almost same tip displacement indicating that at higher airspeeds large deflection effects become significant.

References

Ahmed F. (2006) *Analysis of Data Transfer Methods Between Non-Matching Meshes In Multiphysics Simulations*, Fraunhofer SCAI, 2006.

Aircraft 3D Panel Method web site (2015), *http://www.3dpanelmethod.com*

Akenine-Möller T. (2001) *Fast 3D Triangle-Box Overlap Testing*, Department of Computer Engineering, Chalmers University of Technology, 2001.

Harder, R.L. and Desmarais,R.N. (1972) *Interpolation Using Surface Splines*, Journal of Aircraft, Vol. 9, No. 2, 1972, pp. 189-191.

Hua C. (1990) *An inverse transformation for quadrilateral isoparametric elements: Analysis and application*, Department Of Civil Engineering, The University Of Michigan, 1990.

MSC Nastran *Quick Reference Guide* (2014), MSC.Software Corporation

MSC Nastran *Version 68 Aeroelastic Analysis User's Guide* (2010), MSC.Software Corporation

Palacios R. and Cesnik C. E. S. (2005) *Static Nonlinear Aeroelasticity of Flexible Slender Wings in Compressible Flow,* 46th AIAA/ASME/ASCE/AHS/ASC Structures, Structural Dynamics & Materials Conference, 2005

Patil M. J. and Hodges D. H. (2006) *Flight Dynamics Of Highly Flexible Flying Wings,* Department of Aerospace and Ocean Engineering, Virginia Polytechnic Institute and State University, 2006

Samareh J. A. (2007) *Discrete Data Transfer Technique for Fluid–Structure Interaction*, NASA Langley Research Center, Hampton, 2007.

Smith M. J. (1995) *An evaluation of computational algorithms to interface between CFD and CSD methodologies*, Wright Laboratory, 1995.